Magnetotransport studies of anisotropic scattering in GaAs/AlAs island superlattices

A. Patanè, A. Ignatov,* L. Eaves, P. C. Main, and M. Henini
School of Physics and Astronomy, University of Nottingham, Nottingham NG7 2RD, United Kingdom

E. Schomburg, R. Scheuerer, and K. F. Renk
Institut für Angewandte und Experimentelle Physik, Universität Regensburg, Regensburg 93040, Germany

V. M. Ustinov, A. E. Zhukov, and A. R. Kovsh
A.F. Ioffe-Physico-Technical Institute, Politechnicheskaya 26, St. Petersburg 194021, Russia
(Received 19 February 2002; revised manuscript received 30 April 2002; published 19 August 2002)

We investigate the electronic properties of wide miniband (~100 meV) GaAs/AlAs superlattice structures in which the tunnel barriers are formed from planar arrays of AlAs islands. By studying the effect of an in-plane magnetic field on the miniband conduction, we determine the strength and anisotropy of the rate of electron scattering by the island arrays.

DOI: 10.1103/PhysRevB.66.075325 PACS number(s): 73.21.Cd, 72.80.Ey, 72.10.−d

Semiconductor superlattices (SLs) are of fundamental interest as they provide a means of studying the motion of Bloch electrons in a periodic potential. The nonlinear dependence of the electron drift velocity on applied electric field leads to negative differential conductance in the current-voltage characteristics, $I(V)$.[1,2] At sufficiently large applied bias, the electrical current passing through the superlattice undergoes high-frequency oscillations, driven by traveling dipole domains.[3,4] The frequency of these oscillations is determined by the width of the superlattice miniband and hence by the thickness of the potential barrier.[5] Superlattices with large miniband widths (>10 meV) are of particular interest because of their potential application as new terahertz radiation sources and detectors[6,7] in the fields of communications, astronomy, and biomedical imaging.[8] Recently, negative differential conductance has been observed in the current-voltage characteristics, $I(V)$, of GaAs/AlAs superlattice structures with miniband widths of ~100 meV.[9] In these devices, the mean thickness of the AlAs barrier is reduced to a few atomic layers or even to a fraction of a monolayer (ML). As a result, the continuity of the AlAs layer is broken by the formation of a planar array of Al-rich, (AlGa)As islands embedded within the GaAs matrix. Transmission electron microscopy studies indicate that the in-plane dimensions of the islands are typically a few nanometers.[9] These island SLs are also of potential interest for engineering novel quantum structures, such as one-dimensional coupled quantum-dot devices or superlattices in which the potential is modulated not only along the growth direction but also in the growth plane.[10]

Despite the promise of these novel superlattices, the disorder associated with the partly random array of islands may cause additional elastic scattering of electrons and may lead to a decrease of the miniband electron mobility. In this work, we employ a magnetic field applied parallel to the plane of the island arrays to investigate electron scattering due to the islands. The action of the Lorentz force provides us with a means of tuning both the magnitude and direction of the electron momentum in the plane of the island arrays. By modeling the data in terms of a modified Esaki-Tsu model of the electron motion, we are able to extract the strength and anisotropy of the rate of electron scattering due to the islands.

The samples were grown by molecular beam epitaxy on a heavily Si-doped (n^+), (100)-oriented GaAs substrate. Sample $S1$ consists of 100 periods; each period is formed by 22.5 MLs of GaAs and 0.5 MLs of AlAs. Sample $S2$ consists of 130 periods and each period is made of 14 MLs of GaAs and 2 MLs of AlAs. Using a Kronig-Penney model[11] and the band parameters of the GaAs/AlAs system, we estimate the lowest miniband of the SLs to have widths, Δ, of 105 meV ($S1$) and 120 meV ($S2$). The quantum wells and barriers of the SL were uniformly doped with silicon (the doping concentrations are equal to 8×10^{16} cm^{-3} and 9×10^{16} cm^{-3} for $S1$ and $S2$, respectively), and on the top of each of them, a n^+ Si-doped GaAs cap layer was grown. The samples were processed into circular mesa structures of diameter in the range 10 to 100 μm, with ohmic contacts to the substrate and the cap layer. In the following, we define positive bias with the cap layer biased positive.

Despite the loss of translational symmetry due to the islands, these SL devices have $I(V)$ curves characteristic of Bloch conduction. As shown in Fig. 1, for both samples, the room-temperature $I(V)$ curves exhibit an ohmic region at low bias and a region of negative differential conductance (NDC) at a critical voltage $V_c\sim-1$ V. For $|V|>|V_c|$, the $I(V)$ characteristic of sample $S2$ shows a series of steplike features, which are associated with the formation of traveling domains along the SL axis.[6] The $I(V)$ curves can be described in terms of a modified Esaki-Tsu drift-velocity field characteristic, which takes into account both the elastic and inelastic scattering processes.[12] The calculated $I(V)$ curves reproduce the data with the following values of inelastic (r_i) and elastic (r_e) scattering rates: $r_i=0.8\times10^{13}$ s^{-1} and $r_e=2.0\times10^{13}$ s^{-1} in sample $S1$ and $r_i=0.3\times10^{13}$ s^{-1} and $r_e=1.2\times10^{13}$ s^{-1} in sample $S2$.[6,9] These values are similar to those measured in conventional, narrower miniband GaAs/AlAs superlattices.[5] They indicate that elastic scattering due to collisions of electrons by interface roughness and

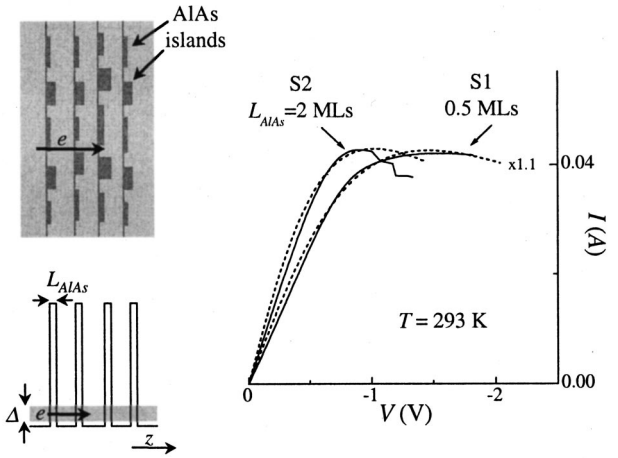

FIG. 1. $I(V)$ at 293 K for samples $S1$ and $S2$. L_{AlAs} is the thickness of the AlAs barriers. Dotted curves are fits to the data (solid curves) by a modified Esaki-Tsu formula (Ref. 12). The left insets show schematically the conduction-band profile (bottom) and a section of the island GaAs/AlAs superlattice (top).

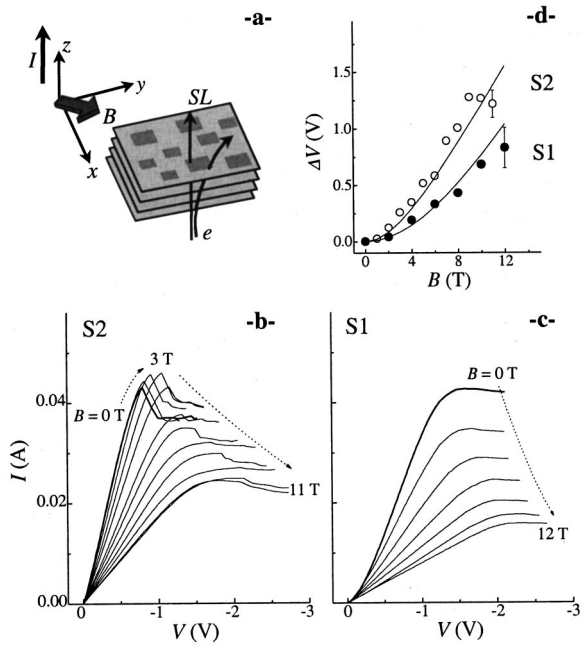

FIG. 2. (a) Geometry of the magnetotransport experiment (B is perpendicular to the current direction). (b) $I(V)$ at 4.2 K vs B for sample $S1$; B is increased in steps of 1 T from 0 to 11 T. (c) $I(V)$ at 4.2 K vs B for sample $S2$; B is increased in steps of 2 T from 0 to 12 T. (d) Voltage shift ΔV of the current peak as a function of B in samples $S1$ and $S2$. Continuous lines are fits to the data.

impurities is comparable with that due to inelastic collisions as a result of the interaction with phonons even at room temperature.

Here we investigate the effect on the motion of the Bloch electrons of a magnetic field B applied perpendicular to the superlattice axis z. In this geometry, the action of the Lorentz force on a Bloch electron tends to increase its momentum components in the (x,y) plane, with a corresponding loss of kinetic energy due to motion along z [see Fig. 2(a)]. This implies that, for increasing B, a larger applied bias is required to sustain miniband conduction along z, thus shifting the peak and associated NDC region in the $I(V)$ curve to higher bias.[13–17] This behavior is shown in Figs. 2(b) and 2(c) for samples $S2$ and $S1$, respectively, and can be described using a semiclassical model of the miniband conduction, which includes the effect of the Lorentz force. The magnetic-field intensity and the strength of electron scattering determine the voltage shift ΔV of the current peak. In particular, at low magnetic fields, i.e., when the cyclotron frequency[18] ω_c is smaller than the scattering frequency $r = r_i + r_e$, the voltage shift is given by

$$\Delta V = V_c \sqrt{1 + \omega_c^2 / r^2} - V_c , \tag{1}$$

where V_c is the critical voltage for NDC at $B=0$. In Fig. 2(d) experimental values of ΔV are fitted to the model with $r = (1.1 \pm 0.1) \times 10^{13}\ \mathrm{s}^{-1}$ in sample $S2$ and $r = (3.3 \pm 0.3) \times 10^{13}\ \mathrm{s}^{-1}$ in sample $S1$. Also, in sample $S2$, the observed nonmonotonic B dependence of the peak value of the current intensity, which shows a maximum at $B = 3$ T, can be ascribed to the interplay between electric and magnetic localization. The electron trajectories undergo a transition from open to closed orbits at a critical magnetic field $B_c = F_c \sqrt{m_{xy}/\Delta} \sim 3$ T, where F_c is the critical electric field for NDC and m_{xy} is the electron effective mass in the (x,y) plane.[15,16]

The in-plane magnetic field provides us with a means of tuning both the magnitude and direction of the electron momentum in the plane of the island arrays. In turn, this affects the miniband current I to an extent that depends on the strength of elastic scattering along the deflection direction of the electron. Therefore, by rotating B in the growth plane (x,y) and measuring $I(B)$ for each rotational angle ϕ, we are able to probe any anisotropy in the scattering process. As shown in Fig. 3, for both samples the current intensity exhibits a clear dependence on ϕ. The angular anisotropy is characterized by a period $\Pi_1 = 180°$, becoming more pronounced with increasing B before saturating close to our highest available fields. The angle of rotation is defined relative to a {110} crystallographic direction in the (001) plane. We also define the {110} direction as the x axis.

In previous experiments on conventional, narrow-miniband SLs,[14] the angular anisotropy was found to have two characteristic periods, $\Pi_1 = 180°$ and $\Pi_2 = 90°$. The anisotropy of the conduction-band structure of the GaAs and AlAs layers can be described in terms of the different in-plane effective masses along the two crystallographic directions [010] and [110] of the (001) plane. As a result of this anisotropy, the current intensity depends on the angle of the in-plane magnetic field with a characteristic period, $\Pi_2 = 90°$.[14,19] In addition, if the AlAs islands at the AlAs/GaAs interface are preferentially elongated along a crystallographic direction (e.g., along the $[1\bar{1}0]$ direction), one can expect an anisotropic scattering of electrons in the growth plane. Therefore, when the magnetic field deflects the electrons in a particular direction, there is a corresponding modulation of current depending on the direction of B with period Π_1

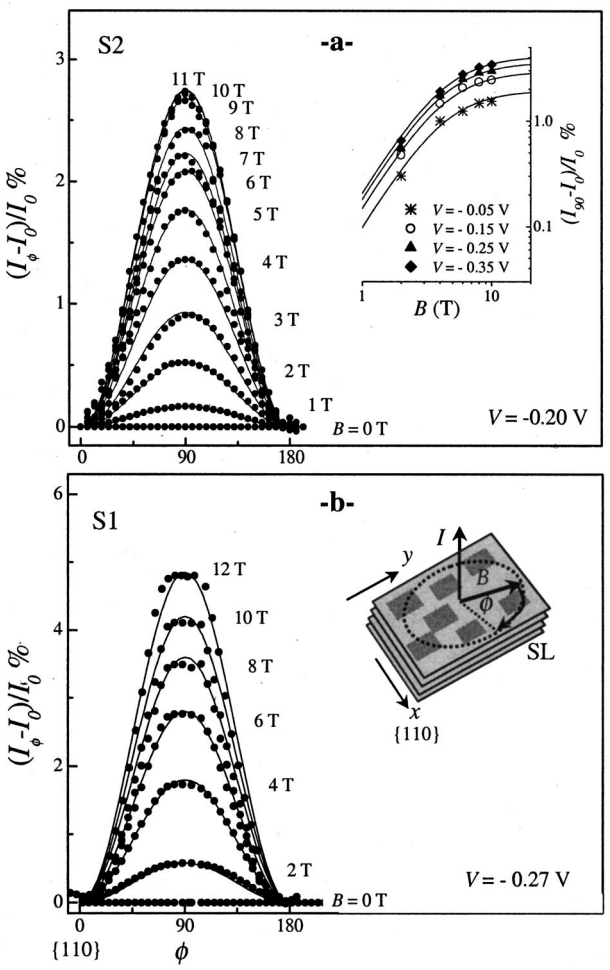

FIG. 3. Dependence of the current I on the angle of rotation ϕ of magnetic field B in the superlattice (SL) plane for sample $S2$ (a) and sample $S1$ (b). ϕ is measured relative to a {110} crystallographic direction in the (001) plane, (x,y). Continuous lines are fits to the data by the curve $A\sin^2\phi$, where A is a constant. The inset on the bottom shows the geometry of the magnetotransport experiment. The inset on the top shows the dependence of $(I_{90}-I_0)/I_0$ on B for different applied biases in sample $S2$.

$=180°$. In our GaAs/AlAs island SLs, the angular dependence of current is characterized by a dominant period $\Pi_1 = 180°$, implying that interface scattering plays the dominant role in these particular structures and that the anisotropy of the effective mass is negligible. This is a reasonable assumption. In fact, due to the high rate of elastic collisions ($r \sim 10^{13}\ s^{-1}$) and corresponding small mean free path of the electrons, $l<10$ nm, the in-plane wave vector acquired by an electron due to the Lorentz force ($k_{xy}=eBl/\hbar<2\times10^8\ m^{-1}$) is much smaller than the width of the Brillouin zone of the crystal ($\sim10^{10}\ m^{-1}$). This implies that, under the conditions of our experiment, our measured values of current are relatively insensitive to the nonparabolicity of the in-plane energy dispersion curves at large values of k_{xy}.

In contrast to previous work,[14] our data also indicate that the anisotropy of the current intensity has a strong dependence on the magnitude of B. Figure 4 shows the B dependence of the angular anisotropy, α, defined according to the relation $\alpha=(I_{90}-I_0)/I_0$, where $I_{90(0)}$ is the current measured for $\phi=90°(0°)$, for samples $S1$ and $S2$. In both samples, α initially increases with increasing B and tends to saturate at the highest magnetic fields. As discussed below, this dependence can be used to probe the strength and in-plane anisotropy of the elastic scattering associated with the AlAs islands.

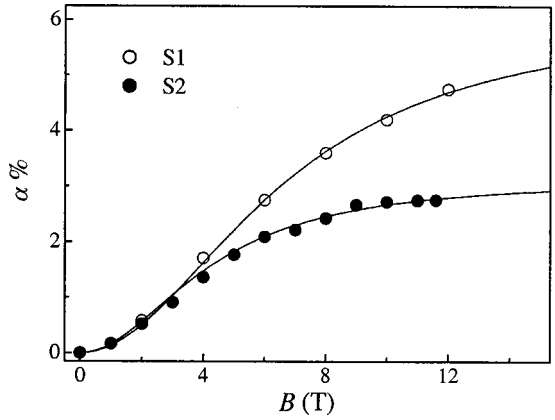

FIG. 4. Dependence of $\alpha=(I_{90}-I_0)/I_0$ on B, for samples $S1$ ($V=-0.27$ V and $T=4.2$ K) and $S2$ ($V=-0.20$ V and $T=4.2$ K). $I_{90(0)}$ is the current measured for $\phi=90°(0°)$. Continuous lines are fits to the data using Eq. (2).

To explain the data shown in Figs. 3 and 4, we consider a semiclassical model of the miniband conduction and assume an anisotropic scattering rate r in the SL plane (x, y), i.e., $r_x>r_y$. This model describes the relaxation rate of the average velocity due to elastic (e) and inelastic (i) scattering processes, i.e., $r_x=r_i+r_{ex}$. We assume that the inelastic processes are isotropic. In the linear regime, the miniband current depends on the intensity and direction of magnetic field according to the relation

$$I_\phi=I_0\left(1+\frac{\delta r}{r_y}\frac{\tilde{B}^2}{1+\tilde{B}^2}\sin^2\phi\right), \qquad (2)$$

where $\tilde{B}=\omega_c/\sqrt{r_z r_y}$, $\omega_c=eB/\sqrt{m_0 m_{xy}}$,[18] r_z is the scattering rate for electron motion along z, and $\delta r=r_x-r_y$. Further details of our model are given in the Appendix.

Equation (2) shows that (i) the current is angle modulated with period $\Pi_1=180°$ and reaches its minimum value I_0 when B is directed along the x axis, corresponding to electrons deflected along the direction (y) of minimum scattering frequency; (ii) at a fixed ϕ, the quantity $\alpha=(I_\phi-I_0)/I_0$ increases with increasing $\tilde{B}$ (or B) and saturates at the value $(\delta r/r_y)\sin^2\phi$.

As shown in Fig. 4, the predicted dependence of α on B describes our data very well. This variation can be understood in terms of the interplay between the action of the Lorentz force, which deflects the electron trajectory away from the SL axis, and the scattering by the AlAs islands, which tends to randomize the electron motion. If the scattering frequency is high compared with the cyclotron frequency ($\tilde{B}\ll1$ or small B), the electron motion in the (x,y) plane is randomized and the current along z is not affected by the

anisotropy of the scattering ($\alpha \sim 0$). In contrast, in the opposite regime of low scattering rates and/or large magnetic field, the electron trajectory is deflected ballistically along a defined direction in the SL plane. This has the effect of reducing the miniband current to an extent that depends on the scattering rate along the deflection direction of the electron. In this regime, which occurs at higher magnetic fields for higher scattering rates, α is independent of B and is equal to $(\delta r/r_y)\sin^2\phi$.

The above discussion indicates that a fit to the data of Fig. 4 by Eq. (2) allows us to measure the average scattering frequency, $\bar{r}=\sqrt{r_z r_y}$, and the in-plane transport anisotropy between different crystallographic directions, $\delta r/r_y$. Equation (2) reproduces our data with fitting parameters $\bar{r}$ and $\delta r/r_y$, which differ for samples $S1$ and $S2$. We find that $\delta r/r_y$ is equal to 6% and 3%, in samples $S1$ and $S2$, respectively. The uncertainty in determining α at a given bias is small ($\pm 0.1\%$). However, the weak dependence of α on bias introduces an additional uncertainty of $\pm 1\%$. Although the difference in the value of α between the two samples is small, it is significant, as it is larger than the estimated uncertainty. In particular, the anisotropy of the elastic processes is described by $\alpha^* = \delta r/r_{ey} = \alpha(1 + r_i/r_{ey})$. By considering the scattering rates given in Refs. 6 and 9, we find that α^* is equal to 8% and 4%, in samples $S1$ and $S2$, respectively. This indicates that the in-plane scattering anisotropy is larger in sample $S1$ and suggests that the thin AlAs layers ($=0.5$ MLs) deposited in this type of structure favor a stronger anisotropy in the morphological properties of the AlAs islands. The origin of this anisotropy may be related to the nonequivalence of the $[1\bar{1}0]$ and [110] crystallographic directions due to a lower diffusion barrier for atoms along the $[1\bar{1}0]$ direction[20] and different reactivity of step edges along the two directions.[21] We believe that these effects become particularly important when a small amount of material, e.g., one atomic layer or less, is deposited. Under these conditions, the growth becomes more sensitive to kinetic processes. Consistent with this, we also find that the average scattering rate is significantly higher in sample $S1$ [$\bar{r}=(2.3 \pm 0.2)\times 10^{13}\ \mathrm{s}^{-1}$] than in sample $S2$ [$\bar{r}=(1.2\pm 0.1)\times 10^{13}\ \mathrm{s}^{-1}$]. The higher scattering rate measured in sample $S1$ is reflected in the fact that α tends to saturate at higher magnetic fields ($B>12$ T) than in sample $S2$ ($B>8$ T). In sample $S1$, the sub-ML deposition of the AlAs barrier generates an in-plane distribution of disconnected (AlGa)As islands, with Al composition and/or size varying in the SL plane.[9] In sample $S2$, the thicker AlAs coverage ($=2$ MLs) is expected to produce more homogeneous AlAs barriers and a corresponding lower scattering rate. The values of $\bar{r}$ derived from the fits based on Eq. (2) agree with the typical scattering rates, $r=r_i+r_e$, derived from the analysis of the $I(V)$ curves at $B=0$ using the modified Esaki-Tsu velocity-electric field characteristic[6,9] and the voltage shift with B of the current peak [see Fig. 2(d)]. The agreement between these independent estimates supports further the validity of our model of the magnetotransport properties of these island SL structures.

In conclusion, we have investigated the electronic properties of wide miniband GaAs/AlAs superlattice devices in which the planar translational symmetry of the thin (~ 1 atomic layer) tunnel barriers is broken by the formation of AlAs islands. By studying the effect of an in-plane magnetic field on the $I(V)$ characteristic, and by modeling the angular dependence of current, we have determined the scattering rate of the Bloch electrons, including the anisotropy of the elastic scattering from the island array.

This work was supported by the Engineering and Physical Sciences Research Council (United Kingdom) and by the Deutschen Forschungsgemeinschaft (Germany). One of us (A.I.) gratefully acknowledges support from the Royal Society (United Kingdom) and from the Graduiertenkolleg ''Non-linearity and non-equilibrium in condensed matter'' at the University of Regensburg (Germany).

APPENDIX

We use a semiclassical model to describe the electron miniband conduction along the SL axis, z, in the presence of an electric field $\boldsymbol{E}=(0, 0, E_z)$ along z and a magnetic field $\boldsymbol{B}=(B_x, B_y, 0)$ in the SL plane (x,y). The average energy due to motion along z, $\bar{\varepsilon}_z(t)$, and the average velocity $\bar{v}=(\bar{v}_x, \bar{v}_y, \bar{v}_z)$ are derived by solving the following equations:

$$\frac{d\bar{v}_x}{dt} = -\frac{eB_y}{m_{xy}}\bar{v}_z - r_x\bar{v}_x, \tag{A1}$$

$$\frac{d\bar{v}_y}{dt} = \frac{eB_x}{m_{xy}}\bar{v}_z - r_y\bar{v}_y, \tag{A2}$$

$$\frac{d\bar{v}_z}{dt} = \frac{1}{m_z(\bar{\varepsilon}_z)}[eE_z + eB_y\bar{v}_x - eB_x\bar{v}_y] - r_z\bar{v}_z, \tag{A3}$$

$$\frac{d\bar{\varepsilon}_z}{dt} = \bar{v}_z[eE_z + eB_y\bar{v}_x - eB_x\bar{v}_y] - r_i(\bar{\varepsilon}_z - \varepsilon_z^T), \tag{A4}$$

where $r_{x,y,z}$ is the relaxation rate of the average velocity along x, y, and z, which includes the rate of energy relaxation, r_i, and of elastic scattering, $r_{ex,ey,ez}$ ($r_{x,y,z}=r_i + r_{ex,ey,ez}$), m_{xy} is the electron effective mass in the SL plane, $m_z(\varepsilon_z)=m_0/(1-2\varepsilon_z/\Delta)$ is the energy-dependent electron effective mass along z, $m_0=2\hbar^2/\Delta d^2$, Δ and d are the miniband width and the period of the SL, respectively, and ε_z^T is the thermal energy of the electrons.

The steady-state solution of Eqs. (A1)–(A4) yields the following cubic equation for the electron velocity along z, $\bar{v}_z$:

$$\omega_c^4 T^2(\phi)\left(\frac{\overline{v_z}}{v_0}\right)^3 - 2\omega_B\omega_c^2 T(\phi)\left(\frac{\overline{v_z}}{v_0}\right)^2 + [\omega_c^2 T(\phi) r_i + \omega_B^2 + r_z r_i]\left(\frac{\overline{v_z}}{v_0}\right) = \omega_B r_i, \tag{A5}$$

where $\omega_c = eB/\sqrt{m_0 m_{xy}}$ is the cyclotron frequency, $\omega_B = eE_z d/\hbar$ is the Bloch frequency, ϕ is the angle between the magnetic field direction and the x axis, $v_0 = \Delta d/2\hbar$, and

$$T(\phi) = \frac{\sin^2\phi}{r_x} + \frac{\cos^2\phi}{r_y}.$$

For $\omega_B \ll \sqrt{r_i r_z}$, i.e., in the regime of low applied biases, and for $k_B T \ll \Delta$, $\overline{v_z}$ depends on the direction of magnetic field according to the relation

$$\overline{v_z}(\phi) = \overline{v_z}(0)\left(1 + \frac{\delta r}{r_y}\frac{\tilde{B}^2}{1+\tilde{B}^2}\sin^2\phi\right), \tag{A6}$$

where $\delta r = r_x - r_y$ and $\tilde{B} = \omega_c/\sqrt{r_z r_y}$.

Finally, since the miniband current I is proportional to $\overline{v_z}$, we model the angular dependence of current by the relation

$$I_\phi = I_0\left(1 + \frac{\delta r}{r_y}\frac{\tilde{B}^2}{1+\tilde{B}^2}\sin^2\phi\right). \tag{A7}$$

*Also at Institut für Angewandte und Experimentelle Physik, Universität Regensburg, D-93040 Regensburg, Germany. Permanent address: Institute for Physics of Microstructures, Russian Academy of Sciences, 603600 Nizhny Novgorod, Russia.

[1] L. Esaki and R. Tsu, IBM J. Res. Dev. **14**, 61 (1970).

[2] For a review, see H. T. Grahn, *Semiconductor Superlattices: Growth and Electronic Properties* (World Scientific, Singapore, 1995).

[3] H. Le Person, C. Minot, L. Boni, J. F. Palmier, and F. Mollot, Appl. Phys. Lett. **60**, 2397 (1992).

[4] K. Hofbeck, J. Grenzer, E. Schomburg, A. A. Ignatov, K. F. Renk, D. G. Pavelev, Y. Koschurinov, B. Melzer, S. Ivanov, S. Schaposchnikov, and P. S. Kopev, Phys. Lett. A **218**, 349 (1996).

[5] E. Schomburg, T. Blomeier, K. Hofbeck, J. Grenzer, S. Brandl, I. Lingott, A. A. Ignatov, K. F. Renk, D. G. Pavel'ev, Y. Koschurinov, B. Y. Melter, V. M. Ustinov, S. V. Ivanov, A. Zhukov, and P. S. Kop'ev, Phys. Rev. B **58**, 4035 (1998).

[6] E. Schomburg, M. Henini, J. M. Chamberlain, D. P. Steenson, S. Brandl, K. Hofbeck, K. F. Renk, and W. Wegscheider, Appl. Phys. Lett. **74**, 2179 (1999).

[7] F. Klappenberger, A. A. Ignatov, S. Winnerl, E. Schomburg, W. Wegscheider, and K. F. Renk, Appl. Phys. Lett. **78**, 1673 (2001).

[8] S. W. Smye, J. M. Chamberlain, A. J. Fitzgerald, and E. Berry, Phys. Med. Biol. **46**, R101 (2001).

[9] E. Schomburg, S. Brandl, K. F. Renk, N. N. Ledentsov, V. M. Ustinov, A. E. Zhukov, A. R. Kovsh, A. Y. Egorov, R. N. Kyutt, B. V. Volovik, P. S. Kop'ev, Z. I. Alferov, A. Rosenauer, D. Litvinov, D. Gerthsen, D. G. Pavel'ev, and Y. I. Koschurinov, Phys. Lett. A **262**, 396 (1999).

[10] H. Sakaki, Jpn. J. Appl. Phys. **28**, L314 (1989).

[11] G. Bastard, *Wave Mechanics Applied to Semiconductor Heterostructures*, Les Editions de Physique (Halsted Press, Paris, 1988).

[12] A. A. Ignatov, E. P. Dodin, and V. I. Shashkin, Mod. Phys. Lett. B **5**, 1087 (1991).

[13] F. Elsholz, A. Wacker, E. Scholl, M. Kast, G. Strasser, and E. Gornik, Phys. Rev. B **63**, 033312 (2000).

[14] F. Aristone, J. F. Palmier, P. Gassot, J. C. Portal, and F. Mollot, Appl. Phys. Lett. **67**, 2916 (1995).

[15] A. Sibille, J. F. Palmier, A. Celeste, J. C. Portal, and F. Mollot, Europhys. Lett. **13**, 284 (1990).

[16] H. J. Hutchinson, A. W. Higgs, D. C. Herbert, and G. W. Smith, J. Appl. Phys. **75**, 320 (1994).

[17] E. H. Cannon, F. K. Kusmartsev, K. N. Alekseev, and D. K. Campbell, Phys. Rev. Lett. **85**, 1302 (2000).

[18] The cyclotron frequency is given by $\omega_c = eB/\sqrt{m_z m_{xy}}$, where m_{xy} and m_z describe the effective mass of the electron in the (x,y) plane and along the superlattice axis z, respectively. Near the bottom of the miniband, $m_z = m_0 = 2\hbar^2/\Delta d^2$, where d is the superlattice (SL) period and Δ is the SL miniband width. m_0 is equal to $0.034m$ and $0.061m$ for samples $S1$ and $S2$, respectively, where m is the free electron mass. We assume that m_{xy} is equal to the electron effective mass in the bulk GaAs ($m_{xy} = 0.067m$).

[19] O. H. Hughes, M. Henini, E. S. Alves, M. L. Leadbeater, L. Eaves, M. Davies, and M. Heath, J. Vac. Sci. Technol. B **7**, 1041 (1989).

[20] K. Shiraishi, Appl. Phys. Lett. **60**, 1363 (1992).

[21] Y. Horikoshi, H. Yamaguchi, F. Briones, and M. Kawashima, J. Cryst. Growth **105**, 326 (1990).